ACS APPLIED MATERIALS & INTERFACES

Research Article

www.acsami.org

Graphene-Based Polyaniline Arrays for Deoxyribonucleic Acid Electrochemical Sensor: Effect of Nanostructure on Sensitivity

Tao Yang,* Le Meng, Jinlong Zhao, Xinxing Wang, and Kui Jiao

Key Laboratory of Eco-Chemical Engineering (Ministry of Education), College of Chemistry and Molecular Engineering, Qingdao University of Science and Technology, Qingdao 266042, China

Supporting Information

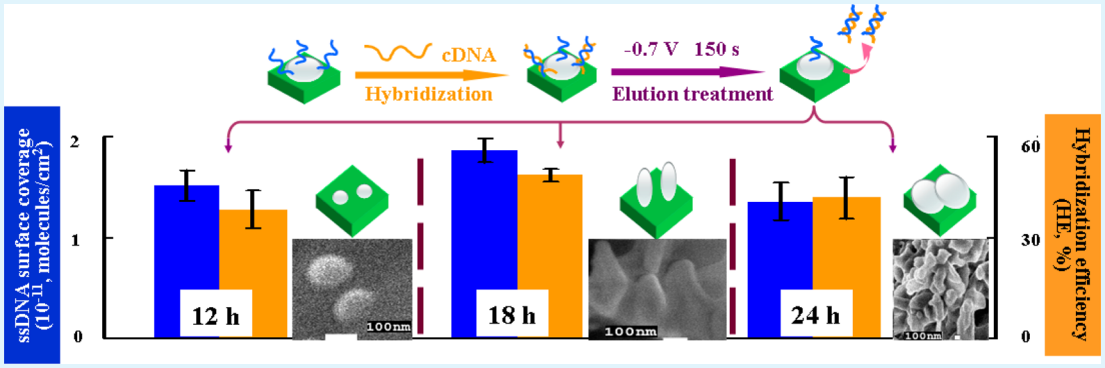

ABSTRACT: DNA detection sensitivity can be improved by carefully controlling the texture of the sensor substrate, which was normally investigated on metal or metal oxide nanostructured platform. Morphology effects on the biofunctionalization of polymer micro/nanoelectrodes have not been investigated in detail. To extend this topic, we used graphene oxide (GNO) as the supporting material to prepare graphene-based polyaniline nanocomposites with different morphologies as a model for comparing their DNA sensing behaviors. Owing to GNO serving as an excellent support or template for nucleation and growth of polyaniline (PANI), PANI nanostructures grown on GNO substrate were successfully obtained. However, if GNO supporting was absent, the obtained PANI nanowires showed a connected network. Furthermore, adjustment of reaction time can be used for dominating the topographies of PANI−GNO nanocomposites, meaning that different reaction times resulted in various formations of PANI−GNO nanocomposites, including small horns (5 and 12 h), vertical arrays (18 h), and nanotips (24 h). The next-step electrochemical data showed that the DNA electrochemical sensors constructed on the different morphologies possessed different ssDNA surface coverage and hybridization efficiency. Compared with other morphologies of PANI−GNO nanocomposite (5, 12, and 24 h), vertical arrays (18 h) exhibited the highest sensitivity (2.08×10^{-16} M, 2 orders of magnitude lower than others). It is can be concluded that this nanocomposite with higher surface area and more accessible space can provide an optimal balance for DNA immobilization and DNA hybridization detection.

KEYWORDS: *nanostructured material, graphene oxide, polyaniline, differential pulse voltammogram, ssDNA surface coverage, hybridization efficiency*

INTRODUCTION

Over the last several years, the electrochemical detection of nucleic acids has been a popular research topic in diseases diagnosis.[1] At the same time, many nanostructured materials (such as nanowires, nanotubes, and nanoparticles) were adopted to fabricate working electrodes, and those works demonstrated that nanostructuring affects the biosensors' capability, owing to their outstanding conductivity, high surface area, and stability.[2] It has been widely known that superior surface area and high conductivity are essential conditions for enhancing sensing behaviors, especially sensitivity.[3] For example, Kelley's group conducted a series of detailed experiments based on Pd nanostructured microelectrodes to explore the interlink between the degree of nanostructuring of a sensor surface and the detection limits toward biomolecular.[2,4,5] Then, they found that the improved detection limit came true when the probe DNA (pDNA) was immobilized on a finely nanostructured electrode surface.[2] In addition, different nanostructured coating materials also can be used to tune sensitivity.[6] Besides other metal nanoparticles, metal oxide nanoparticles, such as zirconia oxide (ZrO_2), have also been used to construct nanostructured microelectrodes for the sensitive DNA electrochemical detection.[7] Based on graphene oxide (GNO) and ZrO_2, our group prepared two kinds of electrochemically reduced graphene oxide (ERGNO) and ZrO_2 hybrids, especially one-step (ZrO_2−ERGNO) and stepwise

Received: July 28, 2014
Accepted: October 23, 2014
Published: October 23, 2014

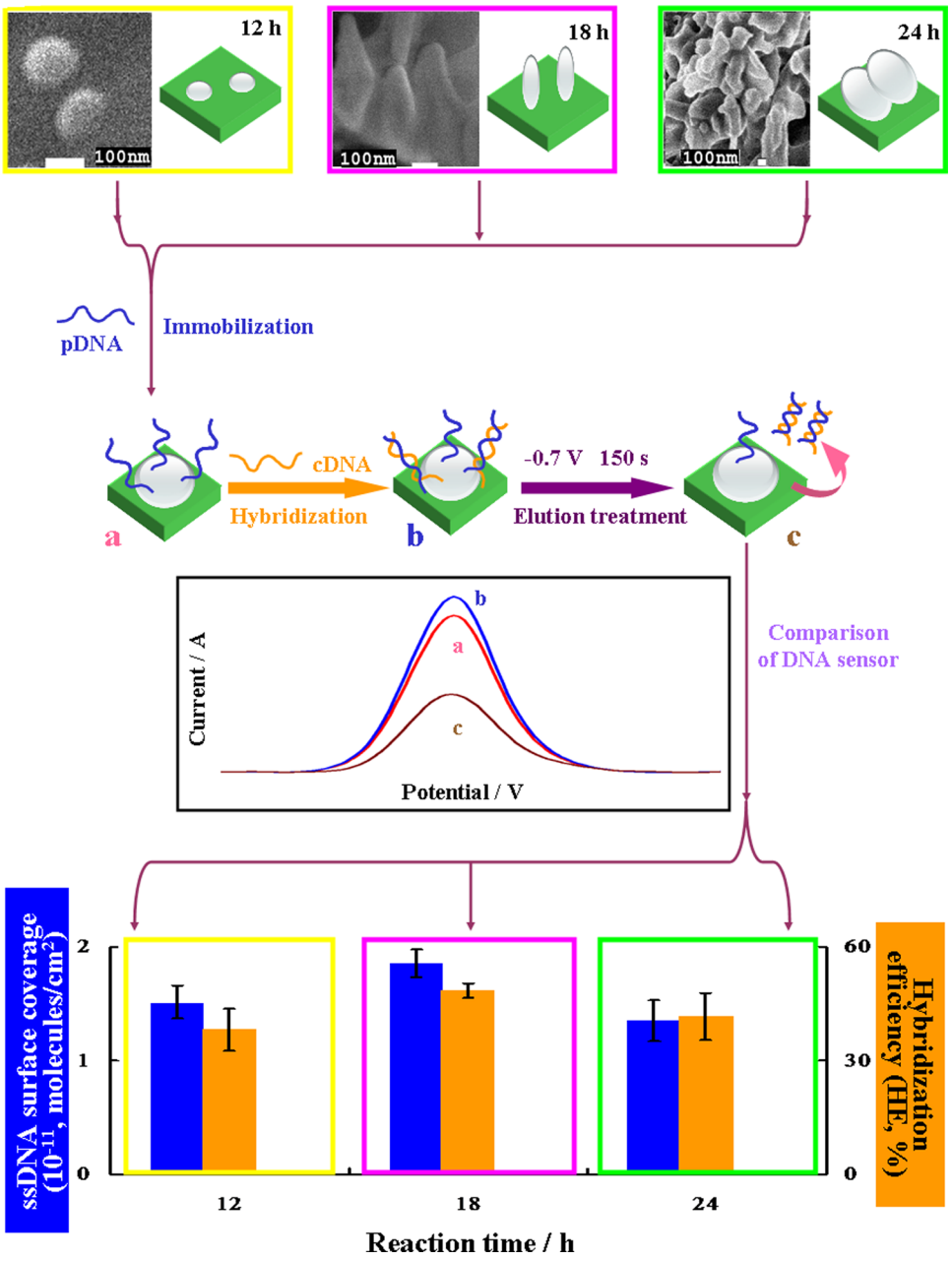

Figure 1. Effect of nanostructure on sensitivity of DNA sensor based on the PANI−GNO. Hybridization efficiency (HE) = ($i_{a\text{ssDNA}} - i_{a\text{dsDNA}}$)/$i_{a\text{ssDNA}}$ × 100; each point is the mean of three measurements; and the error bars correspond to the standard deviation.

(ZrO_2/ERGNO), and compared their hybridization efficiency (HE) for DNA sensing. The results were similar to those reported by Kelley's group. The nanostructured ZrO_2−ERGNO owned better nanostructure and a larger specific surface area than those of microstructured ZrO_2/ERGNO, which enhanced accessibility during pDNA immobilization and hybridization, hence a higher HE.[8] However, the morphology effect of the nanostructured polyaniline (PANI) on sensing behaviors has not yet talked about directly, although it has been widely adopted in DNA detection.[9−15] The DNA biosensor based on the PANI nanotube array could attain similar sensitivity compared with other DNA biosensors that use gold nanoparticles or carbon nanotubes as the substrate.[16] To the best of our knowledge, the morphology effect of varied polyaniline nanostructures on sensitivity of DNA sensors has not yet been studied in detail or directly reported.

Recently, studies exploring novel functional and structural polyaniline nanostructure were focus on the hybrids based on graphene, a novel two-dimensional (2D) nanomaterial.[17−21] A series of approaches, for instance, in situ electropolymerization,[22] simultaneous chemical polymerization,[23,24] and direct mixing of preobtained graphene and PANI,[25] have been adopted to construct nanocomposites using graphene and PANI as the starting materials. Our group took self-doped polyaniline nanofibers intercalated into GNO nanowalls via sonication for highly sensitive and simultaneous detection of bases.[26] In addition, we adopted one-step electrochemical synthesis to obtain the reduced GNO and poly(*m*-aminobenzenesulfonic acid) nanocomposite, rGNO−PABSA, serving as a favorable sensing platform for biomolecule immobilization, especially DNA. It was worth noting that a dramatic improvement in the sensitivity for determination of target

DNA was easily observed, which can be attributed to the synergistic effect of rGNO−PABSA nanocomposite.[27] Compared with the above disorder and random PANI−graphene nanostructures, aligned PANI nanostructures with their excellent electrochemical properties have attracted increasing attention. Xu's group combined 2D GNO nanosheets with one-dimensional (1D) conducting PANI nanowires to construct hierarchical nanocomposites, which possess the synergistic effect of nanocomposites compared with each single monomer.[18] Li et al. fabricated three-dimensional (3D) nanostructure hybrid materials in which uniform aligned PANI nanowire arrays on expanded graphite (EG) nanosheet were obtained.[28] They demonstrated that PANI/EG nanocomposites could serve as excellent supercapacitor electrodes.[28]

In this study, a series of novel nanocomposites, PANI nanostructures, were obtained using a plain and economical chemical synthesis route and GNO substrate. Afterward, the relationship between the nanostructures of PANI−GNO nanocomposite and the sensitivity of DNA biosensor was investigated (Figure 1). From the scanning electron microscopy (SEM) images, the different reaction times (12, 18, and 24 h) directly induce various morphologies of PANI−GNO nanocomposite, which show different surface areas and capture sites and further bring different ssDNA surface coverage and HE (shown in the bottom of Figure 1, histogram). That is to say, the morphology of nanocomposite affects the sensitivity of DNA biosensor. In the histogram in Figure 1, the blue column represents ssDNA surface coverage (for details of the calculation process, see sections S1−S3 in the Supporting Information), while the orange column represents the HE (here, HE = $(i_{a,\mathrm{ssDNA}} - i_{c,\mathrm{dsDNA}})/i_{a,\mathrm{ssDNA}} \times 100$).

EXPERIMENTAL SECTION

Chemicals and Apparatus. A CHI 832 electrochemical workstation (Shanghai CH Instrument Company, China) and a standard three-electrode system including a carbon paste electrode (CPE) or modified electrode as working electrode, a platinum wire auxiliary electrode and a saturated calomel reference electrode (SCE), were used for the electrochemical measurement, as in reference 27. The obtained nanocomposites were characterized by SEM (JSM-6700F, JEOL, Tokyo, Japan).

The following chemicals were obtained: aniline (Tianjin Da Mao Chemical Factory); natural graphite powder (spectral pure, grain size about 30 μm; Sinopharm Chemical Reagent Co., Ltd.); carbon powder (Shanghai Colloid Laboratory); paraffin (Shanghai Hua Ling Healing Appliance Factory); potassium ferricyanide ($K_3[Fe(CN)_6]$, Shanghai No. 1 Reagent Factory, China); potassium ferrocyanide ($K_4[Fe(CN)_6]$, Shanghai Heng Da Chemical Limited Company, China); tris(hydroxymethyl)amminomethane (Tris, Sigma, St. Louis, MO); and methylene blue (MB) and sodium dodecyl sulfate (SDS; Shanghai Reagent Company). All chemicals were analytical grade, and all aqueous solutions were prepared with Aquapro ultrapure water (Ever Young Enterprises Development. Co., Ltd., Chongqing, China) following the same procedure described in reference29.

The 18-base synthetic oligonucleotides used in the experiment were all provided by Shanghai Sangon Biotechnology, Ltd., Co., including pDNA (ssDNA, 5′-TCT CAA TGG CTG CCT CCC-3′), target DNA (complementary DNA (cDNA), namely, an 18-base fragment of PML/RARA fusion gene sequence formed from promyelocytic leukemia (PML) and retinoic acid receptor alpha (RARA), 5′-GGG AGG CAG CCA TTG AGA-3′), single-base mismatched DNA (5′-GGG A**A**G CAG CCA TTG AGA-3), and noncomplementary DNA (ncDNA, 5′-AGT TCA TCC TGC GCT CTT-3′).

First, 100 μL of 1.0×10^{-4} M pDNA were dissolved in 10 mL of Tris−HCl buffer solution (5.0×10^{-3} M Tris−HCl, 0.05 M NaCl, pH 7.0). Then, 100 μL of 1.0×10^{-4} M other aforementioned oligonucleotides sequences (cDNA, single-base mismatched DNA, and ncDNA) were respectively diluted with 10 mL of 2 × sodium saline citrate (2 × SSC, pH 7.0) buffer solution composed of 0.30 M NaCl and 0.030 M sodium citrate tribasic dihydrate ($C_6H_5Na_3O_7 \cdot 2H_2O$). It is worth noting that the obtained homogeneous solutions were all stored at 4 °C before use.

Preparation of Different Platforms. The fabrication of CPE was carried out according to the approach in reference 29. Graphite powder was used as the original material to synthesize graphite oxide (GO) following Hummers' method.[30]

The preparation of PANI−GNO nanocomposite was carried out via chemical polymerization of GNO and aniline monomer with the help of oxidant (ammonium persulfate, APS).[18] A uniform GNO suspension was first obtained by dispersing 36 mg of pure GO in 100 mL of 1 M aqueous perchloric acid solution with the aid of sonication for 30 min. Afterward, 0.465 g of aniline monomer was put into the solution. Additionally, 10 mL of ethanol was added into the reaction solution to avoid the solution being frozen. Then, the obtained solution was stirred and stored at −10 °C for 15 min to form a homogeneous mixture. Meanwhile, the oxidant solution was precooled by dispersing 0.76 g of APS in 10 mL of 1 M aqueous perchloric acid solution, and this solution was cooled at −10 °C. After the rapid addition of APS into the mixture, the resulting mixture was kept for a certain time at −10 °C to realize polymerization. Ultimately, an emerald flocculent precipitate was obtained, filtered, and dried naturally. Through changing the reaction time, a series of morphologies of PANI−GNO nanocomposites were obtained.

In addition, the pure PANI was also chemically synthesized via the same procedure stated as above but without GNO. We added GO to ultrapure water and ultrasonicated the solution for 30 min to get individual GNO.

Five milligrams (5.0 mg) of PANI−GNO nanocomposites was dissolved in 10 mL of ultrapure water, followed by ultrasonication for 30 min, and then a homogeneous suspension was obtained. The bare CPE was covered by 10 μL of the obtained suspension and kept in the air until it naturally dried to form PANI−GNO/CPE. For comparison, we applied the similar procedure mentioned above to prepare GNO/CPE and PANI/CPE.

Immobilization and Hybridization. In this study, the anchoring of ssDNA on working electrode was based on the $\pi-\pi^*$ interaction between conjugated interface and DNA bases according to reference 31. First, 10 μL of Tris-HCl buffer solutions containing 1.0×10^{-6} M ssDNA were dropped onto the nanocomposite modified electrode, air-dried to dryness and rinsed with ultrapure water to drive the unfixed pDNA. DNA hybridization reaction was conducted by dropping 10 μL of 2 × SSC buffer solutions involving 1.0×10^{-6} M cDNA onto the recognition surface. The unhybridized cDNA was removed by leaching the electrode with 0.2% SDS solution, aiming to decrease nonspecific adsorption of cDNA. The effect of elution treatment can be seen in section S4 of the Supporting Information. For the sake of releasing the double-stranded DNA (dsDNA) from the working electrode surface, the electrodes were maintained at −0.7 V for 150 s.[27] Herein, the elution time and elution potential could affect the differential pulse voltammogram (DPV) signals of 2.0×10^{-5} M MB, and the details please see section S5 of the Supporting Information.

Electrochemical Measurements. The following parameters were employed for DPV measurements: pulse amplitude, 50 mV; pulse width, 60 ms; pulse period, 0.2 s. Supporting electrolyte was Britton−Robinson (BR) buffer solution (pH 6.0). To get a reliable response, we soaked the working electrodes in the 2.0×10^{-5} M MB solution for 10 min, and then the signals were recorded.[8]

Cyclic voltammogram (CV) measurements were performed in 1.0×10^{-3} M $K_3[Fe(CN)_6]$ and 1.0×10^{-3} M $K_4[Fe(CN)_6]$ (1:1) solution containing 0.1 M KCl between 0.6 and −0.3 V, as well as in BR buffer solution (pH 6.0) between 0.0 and −0.5 V. The CV scan rate was 0.1 V/s. According to the CV signals of nanocomposites modified electrodes recorded in 1.0×10^{-3} M $K_3[Fe(CN)_6]$ and 1.0×10^{-3} M $K_4[Fe(CN)_6]$ (1:1) solution containing 0.1 M KCl, and signals of 2.0×10^{-5} M MB at the ssDNA modified electrodes, the ssDNA surface coverage was calculated.[27]

The experimental results for each electrode were the average value of three parallel measurements.

RESULTS AND DISCUSSION

Characterization of Hybrids. Figure 2 displays the SEM images of GNO, PANI, and the various PANI−GNO. As shown in Figure 2A, GNO nanosheets are a smooth platform with few folds.[32] After chemical polymerization of the ANI monomers without GNO, the formed PANI displays connected network with average diameter of 40 nm, as shown in Figure 2B. Random connected PANI nanofibers are formed via using aniline micelles as a "soft template" by homogeneous nucleation.[18,33] Furthermore, Figure 2C−F shows how the various morphologies of PANI−GNO nanocomposites (prepared under varying reaction times of 5, 12, 18, and 24 h) are programmed using the axes of reaction time.[18] It can be seen that some small horns appear on the surface of GNO nanosheets with the reaction of 5 h. The small horns begin to grow vertically as the reaction time increases. Once the reaction time reaches 18 h, clear PANI nanofibre arrays on the GNO nanosheets are observed (Figure 2E) with diameters of about 100 nm. The phenomena are similar to the results reported by Xu's group.[18] The aligned PANI nanofiber arrays were formed via chemical polymerization of aniline monomer in the GNO aqueous solution, while random connected PANI nanowires were produced in without GNO aqueous solution. That is to say that GNO served as the support or template for nucleation and growth of PANI.

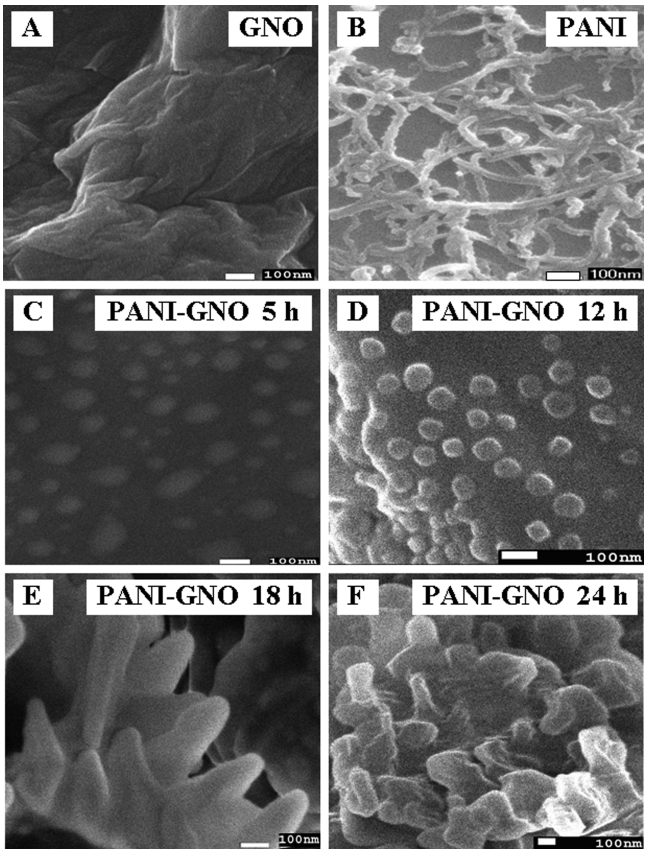

Figure 2. SEM images of (A) GNO; (B) PANI; and PANI−GNO nanocomposites with reaction times of (C) 5, (D) 12, (E) 18, and (F) 24 h in ice bath.

Furthermore, with increasing reaction time, the PANI−GNO nanocomposites interlink to a large-area plate-like structure on bottom with a lot of tips decorated on it. The detail mechanism is not clear now. The results demonstrate that the different reaction times bring various formations of PANI−GNO, including small horns, vertical arrays, and nanotips.

Electrochemical Studies on DNA Immobilization and Hybridization. Controlling the surface textures of nanostructured electrodes can prompt nucleic acid sensors with different sensitivities.[5] The GNO, PANI, and various PANI−GNO nanocomposites exhibit different morphologies, which may further affect ssDNA surface coverage and HE. Here, as a classic electroactive indicator, MB, has been used for monitoring the changes of electrode surface affected by probe immobilization and hybridization.

Figure 3 shows the DPV signals of 2.0×10^{-5} M MB recorded at different nanocomposite-modified electrodes. The representative DPV signals of MB at the GNO/CPE (curve a), ssDNA/GNO/CPE (curve b), and dsDNA/GNO/CPE (curve c) are displayed in Figure 3A. After the ssDNA was immobilized onto the GNO modified electrode surface (ssDNA/GNO), the reduction peak current raised dramatically relative to that of the GNO. Two aspects should be considered to explain the observed this phenomenon. Owing to the unique affinity between MB and the exposed guanine bases of ssDNA, as well as the strong electrostatic interactions between MB cation and electronegative phosphate skeletons of ssDNA, the

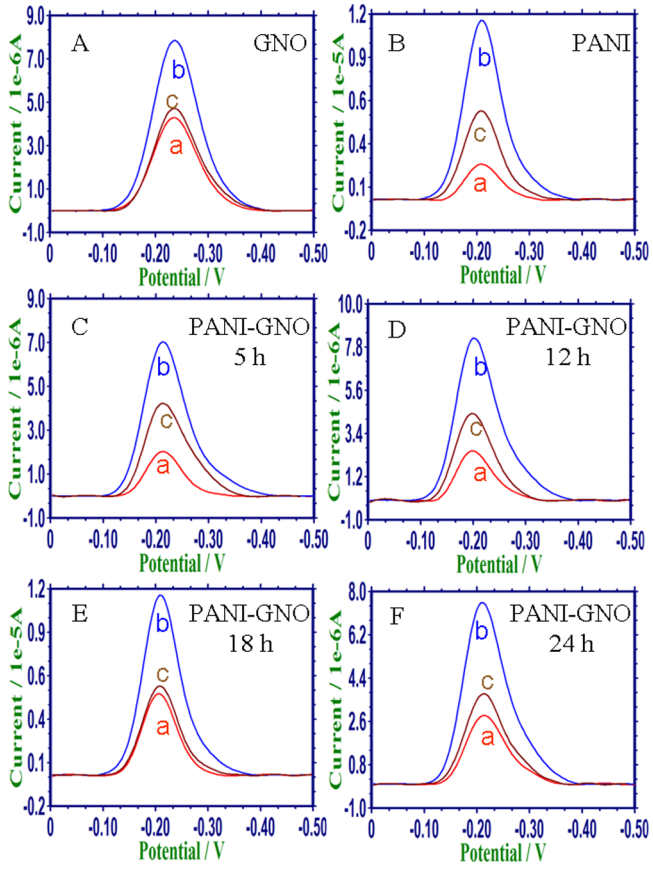

Figure 3. DPV signals of 2.0×10^{-5} M MB of (a) nanocomposites, (b) ssDNA modified CPE, and (c) dsDNA modified CPE. (A) GNO; (B) PANI; and PANI−GNO nanocomposites with reaction times of (C) 5, (D) 12, (E) 18, and (F) 24 h.

dx.doi.org/10.1021/am504998e | ACS Appl. Mater. Interfaces 2014, 6, 19050−19056

greatest MB accumulation happened at GNO layers. That is to say, the increase of reduction peak current can confirm that ssDNA had been successfully bounded to the GNO layers. To get rid of the formed dsDNA from the GNO surface, an elution treatment (−0.7 V voltage for 150 s) was imposed on the modified electrode after the ssDNA hybridized with its cDNA sequence.[34] Then, a significant decrease of the reduction peak current is observed at the dsDNA/GNO/CPE (curve c), which can be ascribed to certain decreasing free guanine bases and negative charge. Additionally, it can be concluded that the binding between the ssDNA and the cDNA is stronger and more stable than the interaction between ssDNA and GNO, which led the formed dsDNA to be released from the conjugated GNO surface.[27,31,35,36] The decrease can be used as strong evidence for identifying the successful hybridization of ssDNA. Moreover, the DPV changes of MB in several other kinds of nanocomposite-modified electrodes show the same tendency (Figure 3B−F).

Figure 4A shows the comparative histograms of the various PANI−GNO nanocomposites obtained from different reaction

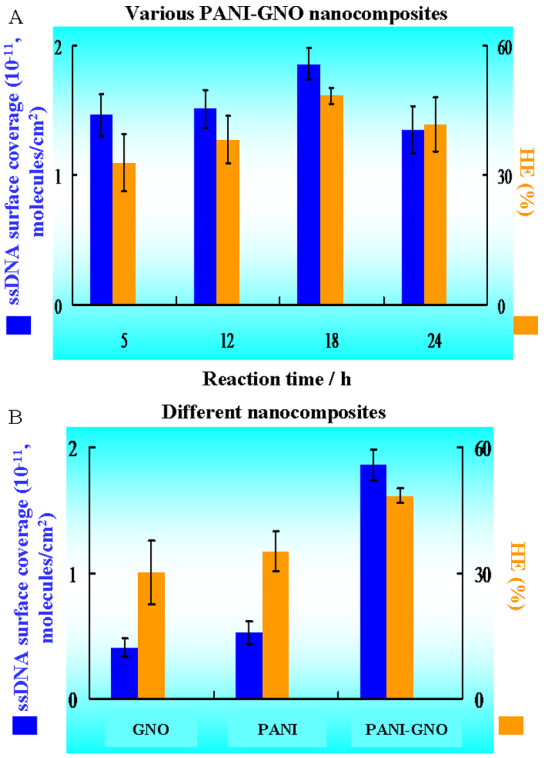

Figure 4. ssDNA (blue column) surface coverage and (orange column) HE. (A) PANI−GNO nanocomposites (5, 12, 18, and 24 h) and (B) different nanocomposites (GNO, PANI, and PANI−GNO).

times. The ssDNA surface coverage and HE increased, accompanied by the increase in the preparation time of PANI−GNO nanocomposite. But after 18 h, ssDNA surface coverage and HE all decreased. For comparison, ssDNA surface coverage and HE of GNO and PANI were also investigated (Figure 4B). It is obvious that the PANI−GNO nanocomposite (reacted for 18 h) modified electrode still exhibits the highest ssDNA surface coverage and HE, which could be attributed to the synergetic effect of PANI and GNO and the fine nanostructure of the PANI−GNO nanocomposite (reacted for 18 h; Figure 2E), allowing more exposed surface area than other nanostructures do. According to Kelley's hypotheses, first, electrodes modified with nanostructured materials own higher surface area and more capture sites, thus inducing higher sensitivity. Second, nucleic acid probe molecules bounded to the surface of electrodes modified with nanostructured materials can provide more accessible space compared with the surfaces of electrodes modified with smoother materials, which induces more efficient and faster binding of analytes.[2]

Detection Comparison of the PML/RARA Gene Sequence. The sensitivity of the electrochemical hybridization detection was measured via hybridization with different concentrations of PML/RARA gene sequence, employing the DPV reduction peak current difference of MB due to the hybridization with different concentrations of cDNA hybridization sequences (namely, Δi_{pc}, $\Delta i_{pc} = i_{pcssDNA} - i_{pcdsDNA}$) as the measurement signal.

After the probe-modified different nanostructured electrodes were hybridized with increasing concentrations of cDNA sequences, the corresponding DPV reduction peak current of MB exhibit decreasing trend, indicating more dsDNA is successfully formed on the modified electrode surface (Figure 5). Variations of DPV reduction peak current differences, Δi_{pc},

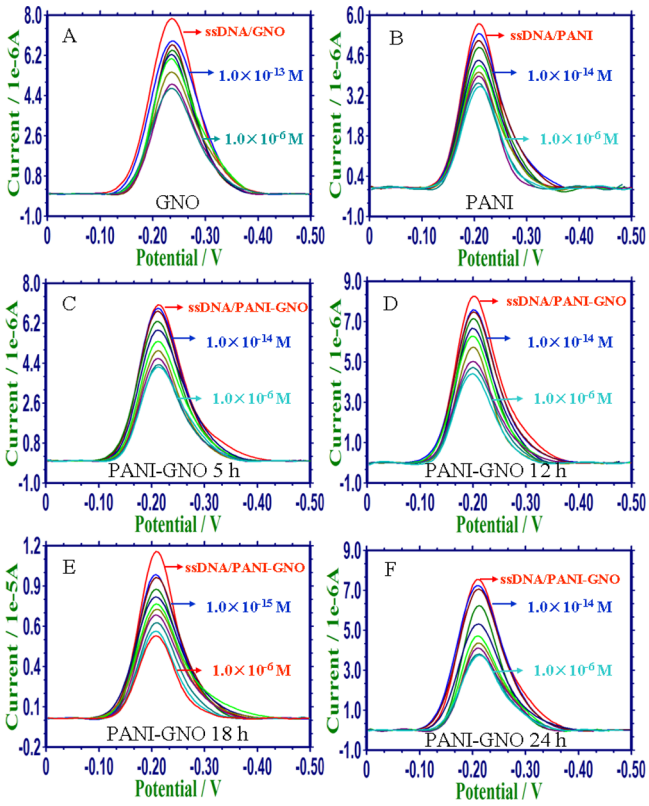

Figure 5. DPV signals of 2.0×10^{-5} M MB at ssDNA modified CPE and after hybridization with different concentrations of PML/RARA fusion gene sequence. (A) GNO; (B) PANI; and PANI−GNO nanocomposites with reaction times of (C) 5, (D) 12, (E) 18, and (F) 24 h.

against cDNA concentrations are plotted in Figure 6. With the increase of reaction time from 5 to 24 h, at 18 h, sensitivity reached its optimum of 2.08×10^{-16} M with a dynamic detection range spanning from 1.0×10^{-15} M to 1.0×10^{-6} M of the target sequences (Figure 6E). The 24 h reaction time did not enhance the electrodes' performances, which suggested the

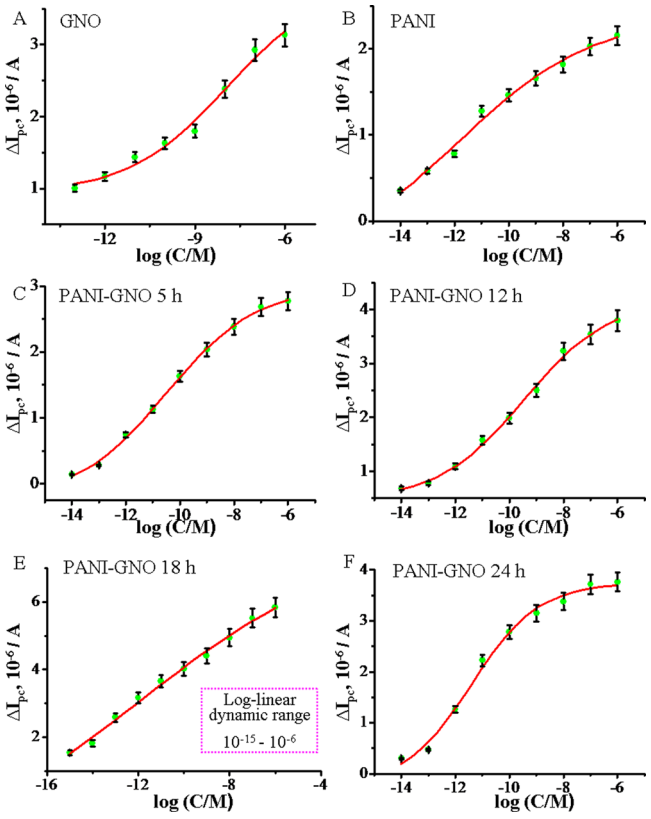

Figure 6. Plot of Δi_{pc} vs the logarithm of PML/RARA gene sequence concentrations. (A) GNO; (B) PANI; and the PANI−GNO nanocomposites with reaction times of (C) 5, (D) 12, (E) 18, and (F) 24 h. The DPV reduction peak current of MB (Δi_{pc}) is the difference between the ssDNA modified electrode and the dsDNA modified electrode.

steric hindrance effect limited the efficiency of the hybridization (Figure 2F).

CONCLUSION

A series of DNA biosensing platforms with different morphologies were developed, and the ssDNA surface coverage and HE using 2.0×10^{-5} M MB as an indicator were compared. On the basis of these comparisons, we confirmed that immobilizing the ssDNA on different morphologies leads to different ssDNA surface coverage, which further affects HE. At the same time, the results showed that the PANI−GNO nanocomposite (reacted for 18 h) owns an optimal balance for DNA immobilization and hybridization detection. This DNA assay was applied to detect PML/RARA gene sequence and then presented relatively wide linear range, low detection limit, and high sensitivity.

ASSOCIATED CONTENT

Supporting Information

Molecules quantity of ssDNA on the electrode surface, microscopic electroactive surface areas of the electrodes, ssDNA surface coverage, effect of elution treatment, optimization of the elution condition, selectivity of the DNA biosensor, and comparison of our works and previous reports, as noted in text. This material is available free of charge via the Internet at http://pubs.acs.org.

AUTHOR INFORMATION

Corresponding Author

*Phone: +86-532-84022665. Fax: +86-532-84023927. E-mail: taoyang@qust.edu.cn.

Notes

The authors declare no competing financial interest.

ACKNOWLEDGMENTS

This work was supported by the National Natural Science Foundation of China (Nos. 21275084 and 41476083), the Doctoral Foundation of the Ministry of Education of China (No. 20113719130001), the Outstanding Adult-Young Scientific Research Encouraging Foundation of Shandong Province (No. BS2012CL013), and the Scientific and Technical Development Project of Qingdao (No. 12-1-4-3-(23)-jch).

REFERENCES

(1) Paleček, E.; Bartošík, M. Electrochemistry of Nucleic Acids. *Chem. Rev.* **2012**, *112*, 3427−3481.
(2) Bin, X. M.; Sargent, E. H.; Kelley, S. O. Nanostructuring of Sensors Determines the Efficiency of Biomolecular Capture. *Anal. Chem.* **2010**, *82*, 5928−5931.
(3) Lan, W. J.; Kuo, C. C.; Chen, C. H. Hierarchical Nanostructures with Unique Y-Shaped Interconnection Networks in Manganese Substituted Cobalt Oxides: The Enhancement Effect on Electrochemical Sensing Performance. *Chem. Commun.* **2013**, *49*, 3025−3027.
(4) Soleymani, L.; Fang, Z. C.; Sun, X. P.; Yang, H.; Taft, B. J.; Sargent, E. H.; Kelley, S. O. Nanostructuring of Patterned Microelectrodes to Enhance the Sensitivity of Electrochemical Nucleic Acids Detection. *Angew. Chem., Int. Ed.* **2009**, *48*, 8457−8460.
(5) Soleymani, L.; Fang, Z. C.; Sargent, E. H.; Kelley, S. O. Programming the Detection Limits of Biosensors Through Controlled Nanostructuring. *Nat. Nanotechnol.* **2009**, *4*, 844−848.
(6) Das, J.; Kelley, S. O. Tuning the Bacterial Detection Sensitivity of Nanostructured Microelectrodes. *Anal. Chem.* **2013**, *85*, 7333−7338.
(7) Cao, Y.; Galoppini, E.; Reyes, P. I.; Duan, Z.; Lu, Y. Morphology Effects on the Biofunctionalization of Nanostructured ZnO. *Langmuir* **2012**, *28*, 7947−7951.
(8) Yang, T.; Guo, X. H.; Kong, Q. Q.; Li, Q. H.; Jiao, K. Comparative Studies on Zirconia and Graphene Composites Obtained by One-Step and Stepwise Electrodeposition for Deoxyribonucleic Acid Sensing. *Anal. Chim. Acta* **2013**, *786*, 29−33.
(9) Tian, S. J.; Liu, J. Y.; Zhu, T.; Knoll, W. Polyaniline/Gold Nanoparticle Multilayer Films: Assembly, Properties, and Biological Applications. *Chem. Mater.* **2004**, *16*, 4103−4108.
(10) Wu, J.; Zou, Y. H.; Li, X. L.; Liu, H. B.; Shen, G. L.; Yu, R. Q. A Biosensor Monitoring DNA Hybridization Based on Polyaniline Intercalated Graphite Oxide Nanocomposite. *Sens. Actuators, B* **2005**, *104*, 43−49.
(11) Arora, K.; Prabhakar, N.; Chand, S.; Malhotra, B. D. *Escherichia coli* Genosensor Based on Polyaniline. *Anal. Chem.* **2007**, *79*, 6152−6158.
(12) Zhang, L. J.; Peng, H.; Kilmartin, P. A.; Soeller, C.; Travas-Sejdic, J. Polymeric Acid Doped Polyaniline Nanotubes for Oligonucleotide Sensors. *Electroanalysis* **2007**, *19*, 870−875.
(13) Arora, K.; Prabhakar, N.; Chand, S.; Malhotra, B. D. Ultrasensitive DNA Hybridization Biosensor Based on Polyaniline. *Biosens. Bioelectron.* **2007**, *23*, 613−620.
(14) Prabhakar, N.; Arora, K.; Singh, H.; Malhotra, B. D. Polyaniline Based Nucleic Acid Sensor. *J. Phys. Chem. B* **2008**, *112*, 4808−4816.
(15) Dhand, C.; Das, M.; Datta, M. B.; Malhotra, D. Recent Advances in Polyaniline Based Biosensors. *Biosens. Bioelectron.* **2011**, *26*, 2811−2821.
(16) Chang, H. X.; Yuan, Y.; Shi, N. L.; Guan, Y. F. Electrochemical DNA Biosensor Based on Conducting Polyaniline Nanotube Array. *Anal. Chem.* **2007**, *79*, 5111−5115.

(17) Novoselov, K. S.; Geim, A. K.; Morozov, S. V.; Jiang, D.; Zhang, Y.; Dubonos, S. V.; Grigorieva, I. V.; Firsov, A. A. Electric Field Effect in Atomically Thin Carbon Films. *Science* **2004**, *306*, 666−669.
(18) Xu, J. J.; Wang, K.; Zu, S. Z.; Han, B. H.; Wei, Z. Hierarchical Nanocomposites of Polyaniline Nanowire Arrays on Graphene Oxide Sheets with Synergistic Effect for Energy Storage. *ACS Nano* **2010**, *4*, 5019−5026.
(19) Zhou, X.; Wu, T.; Hu, B.; Yang, G.; Han, B. Synthesis of Graphene/Polyaniline Composite Nanosheets Mediated by Polymerized Ionic Liquid. *Chem. Commun.* **2010**, *46*, 3663−3665.
(20) Qi, X.; Pu, K. Y.; Zhou, X.; Li, H.; Liu, B.; Boey, F.; Huang, W.; Zhang, H. Conjugated-Polyelectrolyte-Functionalized Reduced Graphene Oxide with Excellent Solubility and Stability in Polar Solvents. *Small* **2010**, *6*, 663−669.
(21) Qi, X.; Pu, K. Y.; Li, H.; Zhou, X.; Wu, S.; Fan, Q. L.; Liu, B.; Boey, F.; Huang, W.; Zhang, H. Amphiphilic Graphene Composites. *Angew. Chem., Int. Ed.* **2010**, *49*, 9426−9429.
(22) Wang, D. W.; Li, F.; Zhao, J. P.; Ren, W. C.; Chen, Z. G.; Tan, J.; Wu, Z. S.; Gentle, I.; Lu, G. Q.; Cheng, H. M. Fabrication of Graphene/Polyaniline Composite Paper via in Situ Anodic Electropolymerization for High-Performance Flexible Electrode. *ACS Nano* **2009**, *3*, 1745−1752.
(23) Al-Mashat, L.; Shin, K.; Kalantar-Zadeh, K.; Plessis, J. D.; Han, S. H.; Kojima, R. W.; Kaner, R. B.; Li, D.; Gou, X. L.; Ippolito, S. J.; Wlodarski, W. Graphene/Polyaniline Nanocomposite for Hydrogen Sensing. *J. Phys. Chem. C* **2010**, *114*, 16168−16173.
(24) Yan, X. B.; Chen, J. T.; Yang, J.; Xue, Q. J.; Miele, P. Fabrication of Free-Standing, Electrochemically Active, and Biocompatible Graphene Oxide−Polyaniline and Grapheme−Polyaniline Hybrid Papers. *ACS Appl. Mater. Interfaces* **2010**, *2*, 2521−2529.
(25) Bai, H.; Xu, Y. X.; Zhao, L.; Li, C.; Shi, G. Q. Non-Covalent Functionalization of Graphene Sheets by Sulfonated Polyaniline. *Chem. Commun.* **2009**, 1667−1669.
(26) Yang, T.; Guan, Q.; Li, Q. H.; Meng, L.; Wang, L. L.; Liu, C. X.; Jiao, K. Large-Area, Three-Dimensional Interconnected Graphene Oxide Intercalated with Self-Doped Polyaniline Nanofibers as a Free-Standing Electrocatalytic Platform for Adenine and Guanine. *J. Mater. Chem. B* **2013**, *1*, 2926−2933.
(27) Yang, T.; Guan, Q.; Guo, X. H.; Meng, L.; Du, M.; Jiao, K. Direct and Freely Switchable Detection of Target Genes Engineered by Reduced Graphene Oxide−Poly(*m*-aminobenzenesulfonic acid) Nanocomposite via Synchronous Pulse Electrosynthesis. *Anal. Chem.* **2013**, *85*, 1358−1366.
(28) Li, Y. Z.; Zhao, X.; Yu, P. P.; Zhang, Q. H. Oriented Arrays of Polyaniline Nanorods Grown on Graphite Nanosheets for an Electrochemical Supercapacitor. *Langmuir* **2013**, *29*, 493−500.
(29) Yang, T.; Meng, L.; Wang, X. X.; Wang, L. L.; Jiao, K. Direct Electrochemical DNA Detection Originated from the Self-Redox Signal of Sulfonated Polyaniline Enhanced by Graphene Oxide in Neutral Solution. *ACS Appl. Mater. Interfaces* **2013**, *5*, 10889−10894.
(30) Du, M.; Yang, T.; Jiao, K. Immobilization-Free Direct Electrochemical Detection for DNA Specific Sequences Based on Electrochemically Converted Gold Nanoparticles/Graphene Composite Film. *J. Mater. Chem.* **2010**, *20*, 9253−9260.
(31) Bonanni, A.; Pumera, M. Graphene Platform for Hairpin-DNA-Based Impedimetric Genosensing. *ACS Nano* **2011**, *5*, 2356−2561.
(32) Yang, T.; Li, Q. H.; Meng, L.; Wang, X. H.; Chen, W. W.; Jiao, K. Synchronous Electrosynthesis of Poly(xanthurenic acid)-Reduced Graphene Oxide Nanocomposite for Highly Sensitive Impedimetric Detection of DNA. *ACS Appl. Mater. Interfaces* **2013**, *5*, 3495−3499.
(33) Zhang, Z. M.; Wei, Z. X.; Wan, M. X. Nanostructures of Polyaniline Doped with Inorganic Acids. *Macromolecules* **2002**, *35*, 5937−5942.
(34) Zhang, X. Z.; Jiao, K.; Liu, S. F.; Hu, Y. W. Readily Reusable Electrochemical DNA Hybridization Biosensor Based on the Interaction of DNA with Single-Walled Carbon Nanotubes. *Anal. Chem.* **2009**, *81*, 6006−6012.
(35) Liu, S.; Wang, L.; Luo, Y. L.; Tian, J. Q.; Li, H. L.; Sun, X. P. Polyaniline Nanofibres for Fluorescent Nucleic Acid Detection. *Nanoscale* **2011**, *3*, 967−969.
(36) Yang, T.; Guan, Q.; Meng, L.; Yang, R. R.; Li, Q. H.; Jiao, K. A Simple Preparation Method for Large-Area, Wavy Graphene Oxide Nanowalls and Their Application to Freely Switchable Impedimetric DNA Detection. *RSC Adv.* **2013**, *3*, 22430−22435.